

Processing and mechanical properties of textured mullite/zirconia composites

Cem Öztürk, Yahya Kemal Tür*

Department of Materials Science and Engineering, Gebze Institute of Technology, P.K. 141, 41400 Gebze-Kocaeli, Turkey

Available online 24 May 2006

Abstract

Textured mullite/zirconia (ZrO_2) composites were prepared from a reactive mixture of alumina (Al_2O_3) and zircon ($ZrSiO_4$) powders together with acicular aluminum borate templates to nucleate and texture mullite grains in the [0 0 1]. Effect of texturing on Young's modulus and strength is investigated by fabricating samples with varying degree of grain orientation by templated grain growth (TGG). It is found that both Young's modulus and strength increases with a better orientation control of mullite grains in the longitudinal direction. The increase in Young's modulus is consistent with the anisotropic elastic properties of mullite crystal. The increase in strength is attributed to the fact that pores are smaller and elongated in the texture direction resulting in smaller defect size. Scanning electron microscopy (SEM) observations indicate that crack propagation at mullite crystals is transgranular.

© 2006 Elsevier Ltd. All rights reserved.

Keywords: Mullite; ZrO_2 ; Composites; Microstructure-final; Mechanical properties

1. Introduction

Material properties are controlled by the microstructure. An effective way of improving the material properties is by combining different materials for the optimum performance; i.e. developing composite materials with a microstructure designed to give mechanical properties suited to the performance requirements.¹ Another way of improving material performance is by orientation control of the individual grains (texture), utilizing the anisotropic properties of the single crystals.² The understanding of the microstructure-property relationship is essential for the improvement/design of ceramic materials for structural applications.

Composite materials containing zirconia (ZrO_2) is extensively studied because martensitic phase transformation of zirconia under applied stress that contributes considerably to the mechanical properties of ceramics.^{3–6} ZrO_2 has superior physical and mechanical properties including high hardness, wear resistance, elastic modulus, and high melting temperature that make it attractive as a structural engineering material.⁷ On the other hand, mullite ceramics have many desirable properties, such as excellent high-temperature strength and creep resistance,

good thermal and chemical stability, low thermal expansion coefficient, and low density.⁸ However, monolithic mullite bodies suffer from low values of bending strength and fracture toughness.⁹ Zirconia could be introduced into mullite matrix by reaction sintering of alumina (Al_2O_3) and zircon ($ZrSiO_4$) at the stoichiometric ratio. In literature, kinetics of phase formation, microstructure evolution, effects of additives and type of starting powders have been extensively studied.^{10–13}

A textured structure can be achieved by templated grain growth (TGG), specifically, by introducing oriented templates into a powder compact to develop a textured microstructure after sintering at elevated temperature.¹⁴ Tape casting is well suited for orienting the templates in the casting direction. In the absence of any significant constraint, mullite has a tendency to grow in the *c* direction leading to the needle-shaped grains. The growth direction of mullite grains can be controlled by orientation of templates in the powder compact by tape casting.

Recently, Duran and Tür showed that the addition of acicular Al-borate whiskers to alumina and zircon powder mixture, employing the tape casting method for green body formation, and sintering at elevated temperature results in the highly textured mullite/zirconia composite structure.¹⁵ In this study, we describe the effect of grain orientation on the mechanical properties of textured mullite/zirconia composites such as Young's modulus and strength. Also, crack growth characteristics of the material are reported. To our knowledge, this is the first report

* Corresponding author. Tel.: +90 262 6051779; fax: +90 262 6538490.
E-mail address: yktur@penta.gyte.edu.tr (Y.K. Tür).

on mechanical properties on the textured mullite/zirconia composites.

2. Experimental procedure

Mullite/zirconia ($3\text{Al}_2\text{O}_3 \cdot 2\text{SiO}_2/\text{ZrO}_2$) composites were prepared from $\alpha\text{-Al}_2\text{O}_3$ (Alcoa, SG3000) and ZrSiO_4 (Eczacıbaşı, Doğa) powders. Ten wt.% [001] aluminum borate ($9\text{Al}_2\text{O}_3 \cdot 2\text{B}_2\text{O}_3$) whiskers (Shikoku Chemical Co.) were used as templates. Three wt.% TiO_2 (Merck, Rutile type) and 1 wt.% MgO (Merck) were added to modify liquid (or glass) phase, based on previous works.¹⁵

A polyvinyl butyral (PVB) was used as a binder and dispersant and a mixture of poly ethylene glycol (PEG) and benzyl butyl phthalate (BBP) was used to modify its plasticity. Appropriate amounts of ZrSiO_4 , Al_2O_3 , TiO_2 and MgO powders were dispersed by ball milling for 24 h in an azeotropic mixture of methyl ethyl ketone (MEK) and ethanol (EtOH) (40/60 vol%) using PVB, PEG and BBP. Al-borate templates were stirred in MEK/EtOH mixture and then introduced into the slurry to avoid template breakage, hereon referred as “intact templates”. For some batches, templates were introduced into the slurry at the beginning of ball milling to break templates and achieve random template alignment in the *a* or *b* direction (hereon referred as “broken templates”). Then, the slurry was stirred for an additional 24 h in a closed beaker for a complete mixing. An ethylene glycol surfactant (Surfynol 104E, Air Products) was added as several drops to remove air bubbles formed during mixing. Excess solvent (MEK/EtOH) was then evaporated until a desired viscosity for tape casting was attained. Tape casting was performed on a glass substrate at a casting speed of ~ 20 cm/s with a blade gap of 200 μm . After drying at room temperature for 24 h, tapes were cut and laminated at room temperature at a pressure of 50 MPa for 3 min. Polymer burnout was carried out by heating samples to 250 °C at 50 °C/h, then to 275 °C at 30 °C/h and finally to 600 °C at 45 °C/h. At each step, there was a dwell time of 1 h. After polymer burnout, samples were sintered at 1450–1550 °C for 4 h with a constant heating rate of 10 °C/min in air.

For microstructural studies, the surfaces of the samples were polished down to 3 μm using diamond paste and then thermally etched 75 °C below the sintering temperature for 45 min in air. Morphological texture was characterized using a scanning electron microscopy (SEM) (Philips XL30 SFEG). Crystallographic texture development was calculated from X-ray diffraction (XRD) (Rigaku Dmax 2200). The amount of texture fraction, Lotgering factor (*f*), for mullite was calculated from Eq. (1)¹⁶

$$f = \frac{P - P^0}{1 - P^0} \quad (1)$$

where *P* and *P*⁰ are $[I_{(001)} + I_{(002)}]/\sum I_{(hkl)}$ in the textured and random sample, respectively. Only mullite peaks were considered in the calculations.

For mechanical tests, samples were prepared with tape casting direction aligned parallel to longitudinal direction,

hereon referred as “parallel composites” and perpendicular to the longitudinal direction, hereon referred as “perpendicular composites”. Parallel samples were prepared with no templates, 10 wt.% broken templates, and 10 wt.% intact templates, whereas perpendicular samples were prepared only with 10 wt.% intact templates. Dimensions of the samples were 1.5 mm × 2 mm × 35 mm (height × width × length). Young’s modulus of samples was measured by the resonance frequency method according to ASTM C1259-94 using a Grindo-Sonic system (Grindo-Sonic MkV, J.W. Lemmens, Belgium). The flexural strength of samples were measured with an electronic universal tester (Model 5569, Instron Ltd.) by a three point bending test with a lower span of 25 mm and crosshead speed of 0.25 mm/min, based on ASTM standard C1 161-90.

3. Results and discussions

Fig. 1 shows the mullite–zirconia phase evolution on *a*–*b* plane as a function of sintering temperature for the samples containing 10 wt.% intact templates. Major peaks are marked on the XRD patterns. Zircon decomposition mainly took place below 1450 °C above which only residual zircon remaining. Zircon further decomposes with the temperature to form final mullite/zirconia. It has been reported that mullite and subsequently mullite/zirconia composite formation was attributed to the presence of both template particles and additives in that additives modified the glass phase providing a path for faster transport of species and isostructural aluminum borate templates served as heteroepitaxial nucleation sites for mullite nucleation and growth.^{15,17} It is also evident that there is only a negligible amount of tetragonal ZrO_2 formation, even though the patterns are from as-sintered surfaces. In other words, almost all ZrO_2 is monoclinic in the composites.

Fig. 2 shows SEM micrographs of the composites which are sintered at 1500 °C with no templates, 10 wt.% broken templates, and 10 wt.% intact templates, respectively. Schematic representation of the each microstructure is also included for visual clarification. Lotgering factors are calculated using Eq. (1). Fig. 2(a) shows that minor texture is present in the sample (*f*=0.15) when no templates were introduced into the slurry,

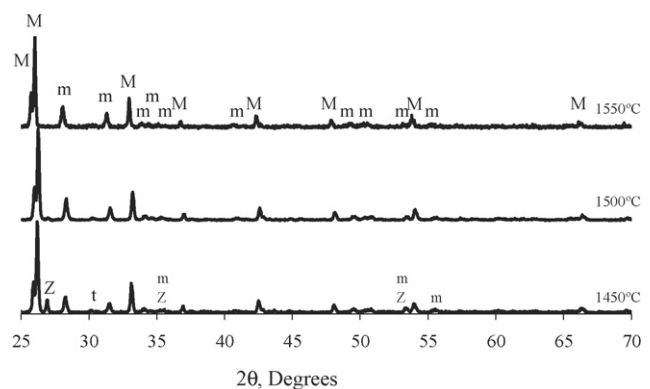


Fig. 1. Phase evolution as a function of sintering temperature for the samples containing 10 wt.% intact templates. M: mullite; m: monoclinic- ZrO_2 ; t: tetragonal- ZrO_2 ; Z: ZrSiO_4 .

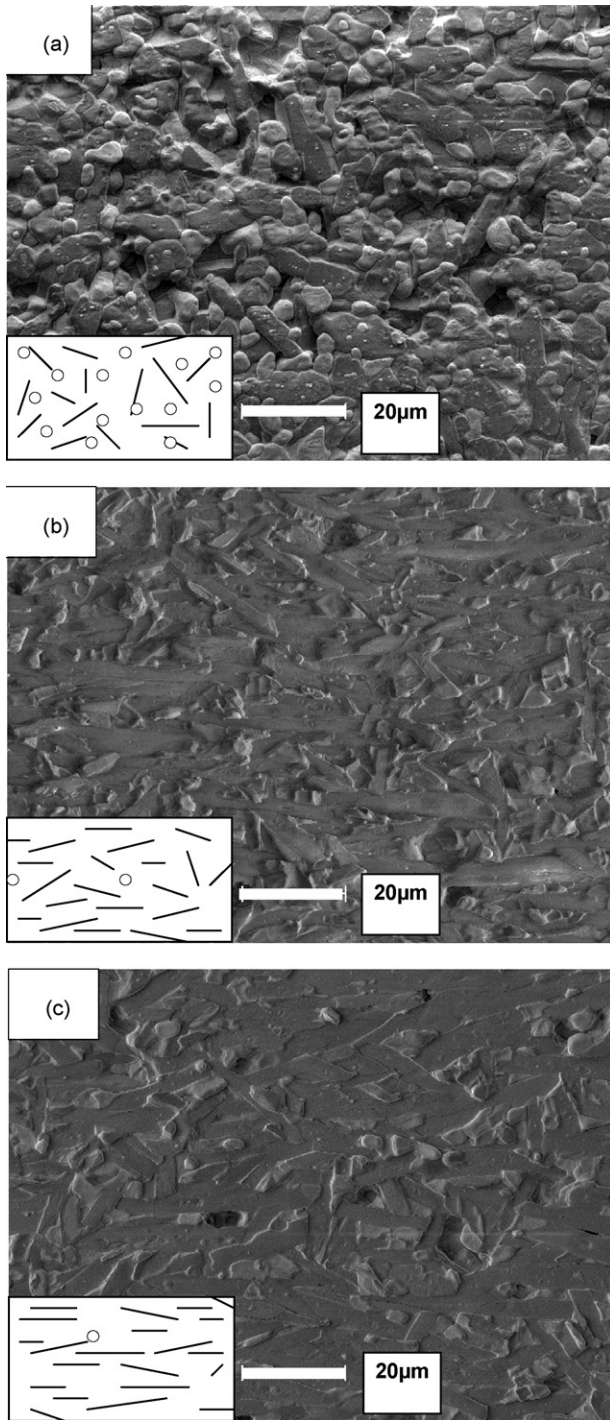


Fig. 2. Texture development in mullite/zirconia composites. (a) No templates ($f=0.15$); (b) 10 wt.% broken templates ($f=0.85$); and (c) 10 wt.% intact templates ($f=0.97$). Inserts show the schematic representation of each microstructure for visual clarification. Tape cast direction is from left to right.

because of the anisotropic growth characteristics of mullite. On the other hand, Fig. 2(b) shows that samples with broken templates have relatively higher textured mullite grains ($f=0.85$) which indicates that acicular shape of the templates still plays a major role in a texture formation. Finally, Fig. 2(c) demonstrates that highly textured ($f=0.97$) mullite grains were achieved for intact templates.

Young's modulus measurements showed that for the composite with no templates E is 164 ± 5 GPa and for the perpendicular composite with intact templates E is 152 ± 5 GPa. On the other hand, for the parallel composite with intact templates, E dramatically increases to 227 ± 5 GPa, which clearly demonstrates the effect of texturing by TGG on E . This increase in E values is attributed to anisotropic structure of mullite crystals, as explained below.

The predicted stiffness evaluated by averaging the stiffness matrix in the longitudinal direction^{18,19} and experimentally measured Young's modulus are compared. Predicted stiffness increases with increasing texture because C_{33} is higher than other elastic constants for mullite crystals. The experimentally measured Young's modulus also increases as the $[001]$ mullite texture fraction (Lotgering factor) in the sample increases from 0.15 to 0.97. Instead of giving absolute values for theoretical and experimentally measured Young's modulus, normalized values may be used. That is, the averaged stiffness, by taking into account the texture fraction and distribution, is divided by 362 GPa (C_{33} for mullite) and the experimentally measured Young's modulus is divided by 230 GPa (slightly higher than experimentally measured value of 227 GPa for highly textured sample, $f=0.97$). Then, it is observed that not only the trend but also the normalized values are very similar. Also, for the perpendicular composites, the low Young's modulus measurements (152 GPa compared 227 GPa) are consistent with the low values of C_{11} and C_{22} in mullite crystal (240 and 285 GPa compared to 362 GPa).

Flexural strength measurements showed that for the composite with no templates σ_f is 175 ± 25 MPa and for the perpendicular composite with intact templates σ_f is 170 ± 25 MPa. On the other hand, for the parallel composite with intact templates, σ_f sharply increases to 300 ± 25 MPa. Similar to the increase in E , TGG induces anisotropy on σ_f . This increase in σ_f values is attributed to the pore size and pore orientation as explained below.

Strength of a ceramic material is a function of its fracture toughness, K_{IC} , and defect size, c .²⁰

$$\sigma_f = \frac{K_{IC}}{Y\sqrt{c}} \quad \text{where } Y \text{ is the geometry factor.} \quad (2)$$

Even though, fracture toughness studies are incomplete, preliminary results indicate that the fracture toughness of the textured composite is not dependent on the crack propagation direction with respect to the mullite grain orientation. This result is supported by SEM observations as well. From Fig. 3 it is seen that cracks propagate as easily through the mullite crystals both parallel and perpendicular to the growth direction, i.e. transgranular crack propagation is the dominant mechanism when crack front reaches a mullite crystal, independent of its orientation. On the other hand, cracks propagate around the zirconia grains, i.e. intergranular crack propagation is the dominant mechanism when crack front reaches a zirconia crystal. Since fracture toughness of the material is not orientation dependent, the discrepancy between the strengths of different orientations should be attributed to the defect size and defect geometry.

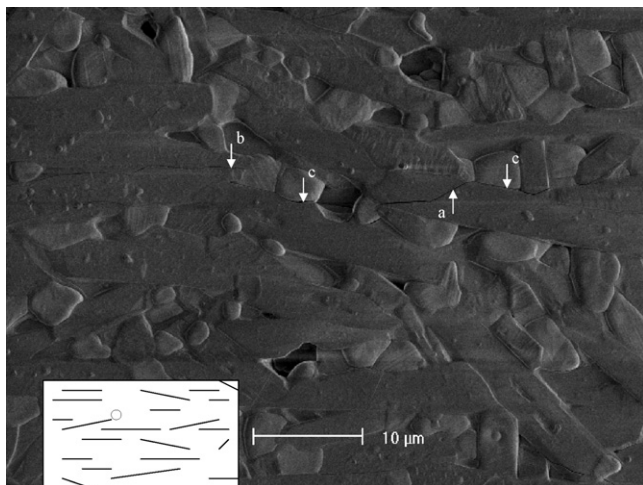


Fig. 3. SEM picture of a sample with $f=0.97$. Arrows labeled as a and b show crack propagation perpendicular to and parallel to the c axis of the mullite crystal, respectively. Arrows labeled as c show the crack propagation around zirconia grains.

In fact, Fig. 3 shows that pores tend to form at the intersection points of textured mullite grains and have a tendency to be elongated in the texture direction. Therefore, detrimental effect of the morphology and alignment of the pore is more pronounced when the stress is applied perpendicular to the texture direction. Therefore, σ_f is much lower for perpendicular composites.

Preliminary results also indicate that the fracture toughness of the textured composite is slightly higher than the un-textured composite, approximately 25%. However, this amount of fracture toughness increase is not enough to explain the two folds of increase in σ_f . Comparison of the morphologies of the un-textured and textured composites (Fig. 2(a and c), respectively), indicate that the pore size is much larger for the un-textured composite. Also, as explained above, pores are elongated parallel to the applied stress in textured composites. Therefore, the increase in strength of textured composite compared to un-textured composite is a result of small defect size achieved by better packing of the grains and better orientation control of the defects.

Above results indicate that textured microstructure in mullite/zirconia composites have beneficial effects on the mechanical properties. One of the expected beneficial effects of texturing was utilizing grain bridging and grain pull out mechanisms during crack propagation, therefore, enhancing the fracture toughness of the material. However, observed crack propagation behavior indicates that these mechanisms are not employed effectively. Also, almost all ZrO_2 is in monoclinic form in all composites, which limits transformation toughening. Work is in progress to further enhance mechanical properties by modifying microstructure (e.g. grain boundary phase) and introducing more tetragonal ZrO_2 (e.g. by adding Yttria).

4. Conclusions

Mullite/zirconia composites with 97% textured mullite grains in $[001]$ ($f=0.97$) were successfully prepared from a reactive powder mixture of alumina and zircon formed by tape cast-

ing. Both E and σ_f increase dramatically with better textured microstructure and better orientation control of mullite grains in the longitudinal direction. E increases from 152 to 227 GPa, and σ_f increases from 170 to 300 MPa for mullite grain orientations perpendicular to and parallel to longitudinal direction, respectively. The increase in E is explained by the anisotropic properties of mullite single crystal. As the mullite grain is oriented better in longitudinal direction, higher elastic properties were achieved because C_{33} in mullite single crystal is higher than other elastic constants. On the other hand, the increase in σ_f is attributed to the pore size and pore geometry of the composite material. As the texture fraction increases, pore size decreases and becomes elongated in the texture direction. However, crack propagation at mullite grains is observed to be transgranular, and almost all zirconia is in monoclinic form.

Acknowledgement

The financial support of the Scientific and Technical Research Council of Turkey (TUBITAK, Project #: 104M229) is greatly acknowledged.

References

- Hull, D. and Clyne, T. W., *An Introduction to Composite Materials (2nd ed.)*. Cambridge University Press, 1996.
- Suvaci, E. and Messing, G. L., Critical factors in the templated grain growth of textured reaction-bonded alumina. *J. Am. Ceram. Soc.*, 2000, **83**, 2041–2048.
- Das, Kaberi and Banerjee, G., Mechanical properties and microstructures of reaction sintered mullite–zirconia composites in the presence of an additive—dysprosia. *J. Eur. Ceram. Soc.*, 2000, **20**, 153–157.
- Yaroshenko, V. and Wilkinson, D. S., Sintering and microstructure modification of mullite/zirconia composites derived from silica-coated alumina powders. *J. Am. Ceram. Soc.*, 2001, **84**, 850–858.
- Mangalaraja, R. V., Chandrasekhar, B. K. and Manohar, P., Effect of ceria on the physical, mechanical and thermal properties yttria stabilized zirconia toughened alumina. *Mater. Sci. Eng.*, 2003, **A343**, 71–75.
- Kaya, C., Kaya, F. and Marsoglu, M., Processing, toughness improvement and microstructural analysis of SiC platelet-reinforced Al_2O_3 :Y-TZP nanoceramic matrix composites. *Mater. Sci. Eng.*, 1998, **A247**, 75–80.
- Hannink, R. H., Kelly, P. M. and Muddle, B. C., Transformation toughening in zirconia-containing ceramics. *J. Am. Ceram. Soc.*, 2000, **83**(3), 461–487.
- Meng, J., Cai, S., Yang, Z., Yuan, Q. and Chen, Y., Microstructure and mechanical properties of mullite ceramics containing rodlike particles. *J. Eur. Ceram. Soc.*, 1998, **18**, 1107–1114.
- Rezaie, H. R., Rainforth, W. M. and Lee, W. E., Fabrication and mechanical properties of SiC platelet reinforced mullite matrix composites. *J. Eur. Ceram. Soc.*, 1999, **19**, 1177–1187.
- Claussen, N. and Jahn, J., Mechanical properties of sintered in situ reacted mullite–zirconia composites. *J. Am. Ceram. Soc.*, 1980, **63**, 228–229.
- Koyama, T., Hayashi, S., Yasumori, A., Okada, K., Schmucker, M. and Schneider, H., Microstructure and mechanical properties of mullite/zirconia composites prepared from alumina and zircon under various firing conditions. *J. Eur. Ceram. Soc.*, 1996, **16**, 231–237.
- Pena, P., Miranzo, P., Moya, J. S. and De Aza, S., Multicomponent toughened ceramic materials obtained by reaction sintering Part 1, ZrO_2 – Al_2O_3 – SiO_2 – CaO system. *J. Mater. Sci.*, 1985, **20**, 2011–2022.
- Descamps, P., Sakaguchi, S., Poorteman, M. and Cambier, F., High temperature characterization of reaction sintered mullite zirconia composites. *J. Am. Ceram. Soc.*, 1991, **74**, 2476–2481.
- Hong, S.-H. and Messing, G. L., Anisotropic grain growth in diphasic-gel-derived titania-doped mullite. *J. Am. Ceram. Soc.*, 1998, **81**, 1269–1277.

15. Duran, C. and Tür, Y. K., Templated grain growth of textured mullite/zirconia composites. *Mater. Lett.*, 2005, **59**, 245–249.
16. Lotgering, F. K., Topotactical reactions with ferrimagnetic oxides having hexagonal crystal structures-1. *J. Inorg. Nucl. Chem.*, 1959, **9**, 113–123.
17. Duran, C. and Tür, Y. K., Phase formation and texture development in mullite/zirconia composites fabricated by reactive templated grain growth. *J. Mater. Sci.*, 2005 [accepted].
18. Messing, G. L., Trolier-McKinstry, S., Sabolsky, E. M., Duran, C., Kwon, S., Brahmroutu, B. *et al.*, Templated grain growth of textured piezoelectric ceramics. *Crit. Rev. Solid State Mater. Sci.*, 2004, **2**, 49–96.
19. Kriven, W. M., Palko, J. W., Sinogeikin, S., Bass, J. D., Sayir, A., Brunauer, G. *et al.*, High temperature single crystal properties of mullite. *J. Eur. Ceram. Soc.*, 1999, **19**, 2529–2541.
20. Brian Lawn, *Fracture of Brittle Solids (2nd ed.)*. Cambridge University Press, 1998.